

Soft Matter

Accepted Manuscript



This is an *Accepted Manuscript*, which has been through the Royal Society of Chemistry peer review process and has been accepted for publication.

Accepted Manuscripts are published online shortly after acceptance, before technical editing, formatting and proof reading. Using this free service, authors can make their results available to the community, in citable form, before we publish the edited article. We will replace this *Accepted Manuscript* with the edited and formatted *Advance Article* as soon as it is available.

You can find more information about *Accepted Manuscripts* in the [Information for Authors](#).

Please note that technical editing may introduce minor changes to the text and/or graphics, which may alter content. The journal's standard [Terms & Conditions](#) and the [Ethical guidelines](#) still apply. In no event shall the Royal Society of Chemistry be held responsible for any errors or omissions in this *Accepted Manuscript* or any consequences arising from the use of any information it contains.

Revealing and tuning the core, structure, properties and function of
polymer micelles with lanthanide-coordination complexes

Junyou Wang,^a Andrea Groeneveld,^a Maria Oikonomou,^a Alena Prusova,^b Henk Van As,^b Jan

W. M. van Lent,^c Aldrik H. Velders^{a,d*}

a: Laboratory of BioNanoTechnology, Wageningen University, Dreijenplein 6, 6703 HB Wageningen, The Netherlands

b: Laboratory of Biophysics and Wageningen NMR Centre, Wageningen University, Dreijenplein 3, 6703 HA Wageningen, The Netherlands

c: Wageningen Electron Microscopy Centre, Wageningen University, Droevendaalsesteeg 1, 6708 PB Wageningen, The Netherlands

d: Interventional Molecular Imaging Laboratory, Department of Radiology, Leiden University Medical Centre, Leiden, The Netherlands.

Keywords: self-assembly, lanthanide, micelles, controlled structures, imaging probes

Abstract

Controlling self-assembly processes is of great interest in various fields where multifunctional and tunable materials are designed. We here present the versatility of lanthanide-complex-based micelles (Ln-C3Ms) with tunable coordination structures and corresponding functions (e.g. luminescence and magnetic relaxation enhancement). Micelles are prepared by charge-driven self-assembly of a polycationic-neutral diblock copolymer and anionic coordination complexes formed by Ln(III) ions and the bis-ligand L_2EO_4 , which contains two dipicolinic acid (DPA) ligand groups (L) connected by a tetra-ethylene oxide spacer (EO_4). By varying the DPA/Ln ratio, micelles are obtained with similar size but with different stability, different aggregation numbers and different oligomeric and polymeric lanthanide(III) coordination structures in the core. Electron microscopy, light scattering, luminescence spectroscopy and magnetic resonance relaxation experiments provide an unprecedented detailed insight in the core structures of such micelles. Concomitantly, the self-assembly is controlled such that tunable luminescence or magnetic relaxation with Eu-C3Ms, respectively, Gd-C3Ms is achieved, showing potential for applications, e.g. as contrast agents in (pre)clinical imaging. Considering the various lanthanide(III) ions have unique electron configurations with specific physical chemical properties, yet very similar coordination chemistry, the generality of the current coordination-structure based micellar design shows great promise for development of new materials such as, e.g., hypermodal agents.

Introduction

Self-assembly that leads to well-defined and tunable structures and functions is of great interest, e.g., in the areas of sensing, catalysis and nanomedicine.^{1,2} Particularly, combining of different functional and structural building blocks, like lanthanide(III) coordination complexes and polymers, allows for integrating the advantages of both worlds into a single composite.^{3,4} Lanthanide(III) compounds possess unique optical and magnetic properties arising from the electron configuration in the partially filled f-shell.⁵ For example, gadolinium(III) complexes with seven unpaired electron spins dramatically decrease the spin-lattice relaxation time of proximate water molecules, leading to their widespread application as MRI contrast agents in medical diagnosis.⁶ Other lanthanide ions, such as europium(III), terbium(III) and erbium(III), are widely used as sensors and optical imaging probes because of their favorable luminescent properties, like long lifetimes, sharp emission bands and high resistance to photo bleaching.^{8,9}

The applications of bare lanthanide(III) coordination structures alone are strongly limited by their constrained size and dynamic metal-ligand exchange properties.¹⁰ On the other hand, designed polymers with versatile structures, lengths, and functional groups have proven to be excellent frameworks for designing drug carriers and localizing inorganic nanoparticles.^{11,12} Therefore, great potential lies in structures that combine the lanthanide coordination structures and polymer building blocks. In fact, several groups have focused on defining the parameters that control coordination stoichiometry, stability and properties. As well-established strategy, chelating ligand groups have been grafted selectively on different polymer blocks that can coordinate lanthanide(III) ions in a self-assembly process yielding micellar structures with

improved magnetic or optical properties depending on the applied lanthanides.¹³⁻¹⁶ Despite these outstanding achievements, controlling the coordination structures and consequently the concomitant functions and properties is a challenge and, to date, possibilities are restricted by designing and synthesizing complex chelating groups/polymers.¹⁷ Of particular interest are the approaches that rely on relatively simple polymers and chelating groups, yet reach good control on the coordination structures and functions. We have recently developed a lanthanide containing coacervate micelles (Ln-C3Ms) from assembly of a polycationic-neutral diblock copolymer with an anionic coordination polymer formed by Ln(III) and a bis-ligand, L₂EO₄, which contains two dipicolinic acid (DPA) groups (L) connected by a tetra-ethylene oxide spacer (EO₄).¹⁸ The formed Ln-C3Ms encapsulate several hundreds of Ln(III) ions in the micellar core, and allow for combining different Ln(III) ions with a controlled tunability on the mixing ratio and corresponding properties. Herein, we exploit a new strategy to tune Ln-C3Ms, by varying the DPA/Ln ratio; this results in Ln-C3Ms with similar size, but with different stability, different numbers of the Ln(III) ions and different coordination structures in the micellar core. Using various complementary techniques, it is possible to obtain detailed insight in the core-structure of these micelles. Concomitantly, tunable luminescence and magnetic relaxation rate with Eu(III), respectively, Gd(III) based micelles are achieved.

Scheme 1 shows the chemical structures of the bis-ligand, L₂EO₄, and the diblock copolymer, P2MVP₄₁-*b*-PEO₂₀₅ (BP). The BP has a linear structure and charge independent of the concentration or solvent conditions, whilst the reversible Ln(III)-L₂EO₄ coordination complexes show structures and overall negative charge that strongly depend on concentration and the ligand/metal ratio, defined as DPA/Ln in this work. Whereas monomeric and short oligomeric complexes are predominantly

present at low concentration of L_2EO_4 and lanthanide, at higher concentration (> 50 mM) polymer networks are formed.^{19, 20} Upon mixing with the cationic-neutral diblock copolymer, P2MVP₄₁-*b*-PEO₂₀₅, the local concentration of L_2EO_4 and lanthanide ions in the micellar core increases to hundreds of millimolar, which dramatically shifts the equilibria of the coordination structures to form coordination polymers.²¹ From previous work on dendrimicelles (i.e. with negatively charged dendrimers in the core of micelles formed with P2MVP₄₁-*b*-PEO₂₀₅), we know that charge and size of core-structures can strongly influence the micelle formation and properties, providing parameters to tune and control the self-assembly.²² In the current study, we systematically investigated the effects of DPA/Ln ratio, from 2 to 3 and 6, on the formation and properties of Ln-C3Ms, observing micelles with different coordination structures in the core and complex charges strongly relying on the DPA/Ln ratio.²³

In a first approximation, assuming that predominantly the DPA and water molecules will be coordinating ligands, basically four different types of Ln(III) complexes can be expected to be present in solution, each of which with a different net charge: $[Ln(DPA)_x(H_2O)_{9-3x}]^{3-2x}$ with x an integer ranging from 0 to 3 (note, DPA represents here one half of the bis-ligand L_2EO_4). In the case of a DPA/Ln ratio of 2, coordination chains with one negative charge per coordination complex/unit are expected in the micelle core.²⁴ Increasing the DPA amount to DPA/Ln ratio of 3, networks are found with three negative charges per coordination complex. At the ratio of 6, predominantly, the mononuclear complex with one Ln(III) and three L_2EO_4 ligands could be expected, the whole structure carries nine negative charges, $[Ln(L_2EO_4)_3]^{9-}$. We hypothesized that the different charges per complex could provide different kinds of micelles (e.g. aggregation numbers). Note that, Scheme 2 represents

the coordination structures in the micellar core and not the free Ln-L₂EO₄ complexes in solution. The coordination complexes discussed here are the expected predominant structures under the designed ratio, other complexes may co-exist due to the dynamic aspects and reversibility of the Ln-DPA coordination bond.²⁵ In fact, and interestingly, we find subtle differences between our hypothesized (Scheme 2, left) and observed (Scheme 2, right) coordination structures in the micelle core as discussed in detail below.

C3Ms normally form optimally around the charge stoichiometry, called PMC (preferred micellization composition) point,²⁶ where the charge compensation is reached completely. To find out the PMC for our Ln-C3M micelles, we titrated the P2MVP_{41-b}-PEO₂₀₅ into Eu-L₂EO₄ solution (20 mM MES buffer at pH 6) under DPA/Eu ratios of 2, 3 and 6; the concentration of Eu(III) was fixed at 0.5 mM, and the bis-ligand concentration varied according to the designed DPA/Eu ratio. Figure 1a shows the light scattering intensity as a function of added amount of BP. For Eu-L₂EO₄ structures at all DPA/Eu ratios, addition of copolymer induces a clear increase of the intensity, suggesting aggregation to occur immediately. The intensity keeps going up with increasing BP and reaches a plateau, the PMC point, at certain amount of BP which strongly depends on the DPA/Eu ratio used. CONTIN analysis (Figure 1b) indicates the Eu-C3Ms are mono-disperse with hydrodynamic radii around 21 nm for DPA/Eu ratios of 2 and 3, and around 24 nm for ratio of 6 (Table 1).

The radii of the micellar cores have been estimated from the Cryo-TEM images (Figure 2) and shell thicknesses were calculated based on the hydrodynamic and core radius (Table 1). Although the size does not vary much for the different DPA/Ln ratios, the composition in the micellar cores changes significantly, as can be seen from the aggregation numbers obtained from the static light scattering data (Table 1, Figure

S3). For micelles with DPA/Eu ratio of 2, we find around 900 Eu(III) ions, 900 L₂EO₄ ligands and 25 P2MVP blocks from BP per micelle core (Table 1). The number of lanthanide ions per micelle decreases rapidly and the number of BP increases steadily upon increasing the DPA/Eu ratio, resulting in about 300 Eu(III) ions and 48 P2MVP blocks in the micellar core for ratio 6, whilst the number of bis-ligand is about 663. Clearly the assembly driven by the electrostatic interactions leads to different combinations of the three components in the core and the final structure is regulated by charge compensation. Importantly, these findings indicate that we can control the lanthanide number (density) and coordination structures (properties) in coacervate micellar cores without changing the micellar size (Figure 3).

As the charge stoichiometry is reached at PMC, based on the consumed amount of BP, we calculated the negative charges per coordination complex/unit of the Eu-L₂EO₄ oligomer/polymer structures. For the DPA/Eu ratios of 2 and 3, coordination complexes are found to have a net negative charge of 1 and 3, respectively, per complex, so corresponding to the expected values based on the $[\text{Ln}(\text{DPA})_x(\text{H}_2\text{O})_{9-3x}]^{3-2x}$ formula (see Table 1). For the DPA/Ln ratio 6, we find the charge numbers per coordination unit to be around 6.2, so lower than expected for $[\text{Ln}(\text{L}_2\text{EO}_4)_3]^{9-}$ (Table 1). As one DPA carries 2 negative charges and one Ln(III) carries 3 positive charges, the 6.2 charge/unit corresponds to a DPA/Ln ratio about 4.6 in the micellar core ($x \cdot 2 + 3 = -6.2$). This deviation indicates that around 12% of the bis-ligand present is not involved in the micelle assembly.

To corroborate the incomplete incorporation of L₂EO₄ in the micelles at DPA/Eu ratio of 6, we ran ¹H-NMR experiments on the micelles to trace the free L₂EO₄ in solution. The protons on the aromatic ring from DPA show a chemical shift around 7.7 ppm, (square area, Figure 4) which is indicative for the free ligand. As shown in Figure 4,

spectra of micelles at 2 and 3 ratios show nothing at 7.7 ppm, confirming all the ligands stay in the micelles. However, the spectrum at 6 ratio gives a clear peak at 7.7 ppm, the amount of free ligand is about 14% as estimated with an internal standard TSP (0 ppm). This value agrees well with the number obtained from light scattering data, confirming there is indeed free ligand at this DPA/Eu ratio.

Further characterization of Eu-C3Ms was performed with luminescence spectroscopy. DPA is a well-known antenna ligand that can sensitize the Eu(III)-luminescence exciting in the UV. However, here direct excitation of the Eu(III) at 395 nm was selected, first, to avoid inner filter effects,²⁷ and, second, because the concentration of Eu(III) was fixed for micelles at all DPA/Eu ratios. Figure 5 shows the emission spectra from Eu-C3Ms at different DPA/Eu ratio, the typical transitions of Eu(III) from 5D_0 to the ground state 7F_J are evident with emissions located at 580 (J = 0), 593 (J = 1), 614 (J = 2), 649 (J = 3), and 688, 693, 703 nm (J = 4).²⁸ Luminescence life time (SI, Figure S6) provides complementary information about the internal coordination structures. Since the micelles contain hundreds of Eu(III) ions in the core, and different coordination structures may co-exist, it is impossible to identify the exact coordination state for each unit. However, one can still estimate the number (q_{average}) of inner sphere H_2O molecules (Table 1, Figure 3), which are the H_2O molecules directly coordinated to the metal center, based on the life times (τ) of micellar solutions in H_2O and D_2O (Figure S6).²⁹ The Eu-C3Ms formed at DPA/Eu ratio of 2 show a q_{average} around 1.2, which is much lower than the expected 3. This difference is most likely due to the ill-defined heterogeneous mixture of possible complexes at this metal-ligand ratio; all complexes of the type $[Ln(DPA)_x(H_2O)_{9-3x}]^{3-2x}$ with x an integer ranging from 0 to 3 might be present, and also coordination of counter ions to the lanthanides might be contributing to the average number observed.

For micelles at DPA/Eu ratio of 3, we find the $\tau_{\text{H}_2\text{O}}$ and $\tau_{\text{D}_2\text{O}}$ are about 1.2 and 2.7 ms, respectively (Table 1), in accordance to reported values for saturated Eu-DPA₃ structures,³⁰⁻³² the q_{average} is ~ 0.27 . Given the high DPA/Eu ratio, no Eu-DPA species are expected and we can consider only the structures Eu(DPA)₂ ($q = 3$) and Eu(DPA)₃ ($q = 0$). Then the q_{average} , of 0.27, suggests around 91% of the Eu(III) to be present as the fully coordinated structures Eu-DPA₃ in the micellar core.³⁰ The q_{average} of the micelles prepared at the DPA/Ln ratio 6 is around -0.1, corresponding to 0 within the error range as suggested in other studies.³³ Hence, all the Eu(III) ions in the micellar core are fully coordinated with three DPA groups. We note that the data fitting and analysis are simplified for such a complex micellar assembly system, still, the numbers are close enough to those from other studies working on Eu-DPA in solution, and nicely complement the results from light scattering and the steady state luminescence.

Luminescence properties (steady-state and life time) strongly depend on the local coordination of the Eu(III) ion, whilst light scattering informs on the charges and aggregation numbers in the micelles and hence indicating the structure of the Eu-L₂EO₄ complexes. Combining the results from both techniques, we conclude the Eu-L₂EO₄ in the micellar core at DPA/Eu ratio of 2 consists of a heterogeneous mixture of different polymeric structures, whilst at the DPA/Eu ratio of 3, practically an ideal network structure is present (Scheme 2). At the DPA/Eu ratio of 6 not (only) the mononuclear $[\text{Ln}(\text{L}_2\text{EO}_4)_3]^{9-}$ is present, but likely several types of multinuclear structures with lower charge-per-complex, such as dimers, trimers and oligomers. Such kind of structures leave part of L₂EO₄ ligands free in solution whilst all Eu(III) ions remain anyways fully coordinated with three DPA groups. Although we cannot define the distribution of different oligomeric structures in the core, interestingly, the

trinuclear $[\text{Ln}_3(\text{L}_2\text{EO}_4)_6]^{19-}$ provides on average 6.3 charges per Ln(III) complex and a DPA/Ln ratio of 4.6 in the core. This corresponds perfectly to the charge neutral DPA/Ln ratio calculated from the DLS data, and hence is presented as the predominant species in the micelle core (Scheme 2).

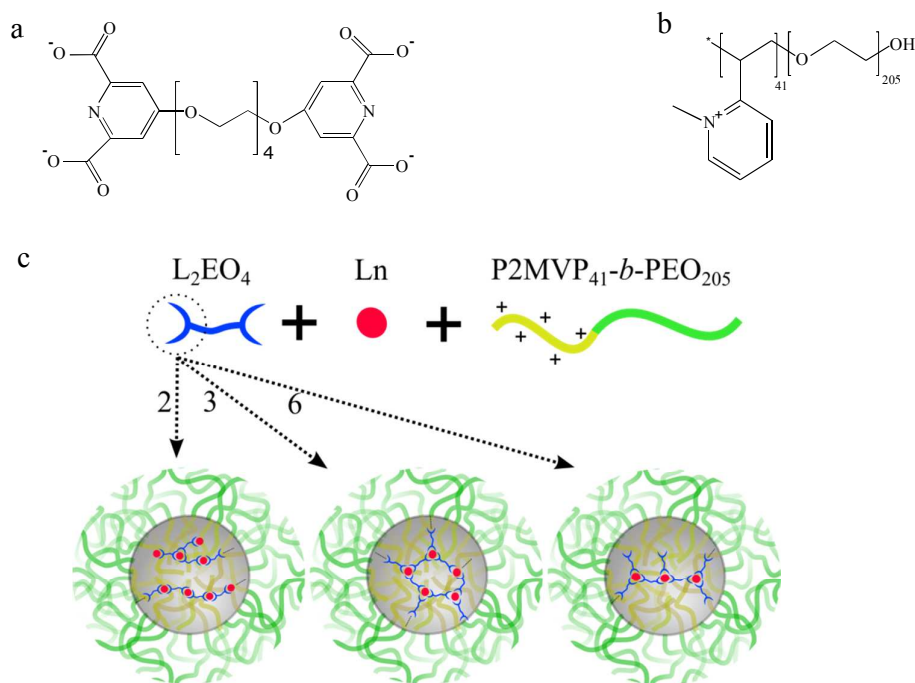
From light scattering and luminescence data, we clearly find a change in the coordination structure and a decrease on the average number of inner sphere water molecules with increasing DPA/Ln ratio. To further validate the general applicability of Ln-C3Ms, we studied both the Eu-C3Ms and Gd-C3Ms for their luminescence, and magnetic relaxation properties, respectively. Eu-C3Ms at all DPA/Ln ratios show the typical sharp-line emission from Eu(III), and the main emission at 614 nm is collected and plotted as a function of DPA/Eu ratio in Figure 6a. Apparently, micelles formed with more ligand involved per Eu(III) ion provide a stronger emission due to the decrease of the luminescence quenching by coordinated water molecules. This is consistent with the observed decay of q_{average} upon increasing the DPA/Ln ratio. With Gd-C3Ms, on the other hand, we expect a decrease of the relaxation rate enhancement upon increasing DPA/Gd ratio, as it is inversely proportional to the number of coordinated water molecules (q_{average}).⁶ As shown in Figure 6b, we indeed see a decrease on the relaxation rate and a clear decay of the contrast on the T_1 -map images at 3 T, the clinically relevant magnetic field strength. These findings corroborate that our method is generally applicable in different lanthanide systems and shows promise for on demand tuning of multi-modal imaging probes. Different imaging modalities have different sensitivities and having tools to adapt the specific modality-related windows for useful and comparable contrast enhancement is of paramount importance. C3Ms are sensitive to ionic strength and dissociate completely above a critical salt concentration (CSC).^{34, 35} We have titrated NaCl into the micellar solution and the

typical titration curve is shown in Figure 7a. The intensity goes down upon increasing salt concentration, and the jump on the decay curve is related to a deformation of the micelles which has been found also in previous studies on C3Ms.^{36, 37} The critical salt concentrations of micelles at different DPA/Eu ratios are plotted in Figure 7b. CSC of micelles at 1/2 is around 150 mM, in the same range as the C3Ms from linear polyelectrolytes,^{35, 37, 38} suggesting the Eu-L₂EO₄ structures in the micellar core may still be mainly the linear coordination polymer structures with a wide distribution. Network structure of Eu-L₂EO₄ polymers with more charges enhance the stability dramatically, the SCS of micelles at DPA/Ln ratio of 3 is found around 650 mM. Interestingly, this number does not decay for Eu-C3Ms at 6. As we believe the mononuclear structure with one Eu(III) and three L₂EO₄ ligands (Scheme 2) cannot form micelles with high stability as much as that of more highly charged networks formed with ratio of 3. This observation confirms that cross-links occur in the micellar core, leading to dimers, trimers and even bigger networks, with concomitant increase of the total negative charges, consequently, a high stability of the micelles.

In conclusion, lanthanide ions provide excellent spies to investigate the core structure of micelles. We have demonstrated a micellar system incorporating tunable lanthanide coordination structures in the micellar core without changing the particle size. Ln-C3Ms form based on the self-assembly of a polycationic-neutral diblock copolymer, P2MVP₄₁-*b*-PEO₂₀₅ and dynamic Ln-L₂EO₄ coordination structures. Upon increasing the DPA/Ln ratio, the coordination structures change from widely distributed chains (2) to well-defined polymeric network structures (3) and eventually to a limited number of oligonuclear structures (6), which corresponds to less and less coordination sites of the Ln(III) ions being occupied by water molecules. This decrease of the inner sphere water molecules induces further a gradual increase of luminescence with Eu-

C3Ms and a clear decrease of the magnetic relaxation rate with Gd-C3Ms, providing a major tool for general application in, e.g., multimodal imaging agents. The overall charge of the coordination structures also varies with changing DPA/Eu ratio, leading to different stabilities of the micelles against salt. Our approach provides a good example how self-assembly can be applied to tune the structure and functions in a facile manner, and may open new way to build up novel sensors or functional materials. The coordination chemistry of the lanthanide(III) ions is very similar which allows to develop general assembling schemes providing compounds with the specific physical-chemical properties selective for the lanthanide(s) chosen. As such, one can envision lanthanide coordination structures could play a big role in the design of hypermodal agents for diagnostic as well as therapeutic applications.^{39, 40}

Scheme 1



Scheme 1: Molecular structures of (a) the ligand L_2EO_4 and (b) $P2MVP_{41}-b-PEO_{205}$ diblock copolymer (BP) and, (c) formation of micelles from $Ln-L_2EO_4$ (Eu(III), Gd(III)) coordination structures and diblock copolymer. The numbers 2, 3, 6 indicate the DPA/Ln ratio in the starting solutions.

Scheme 2

	Designed DPA/Eu & Structure		Observed DPA/Eu & Structure
2		2.1	
3		3.0	
6		4.6	

Scheme 2 Summary of the alternative designed and observed Eu-L₂EO₄ coordination structures and DPA/Eu ratios in the micellar core.

Figure 1

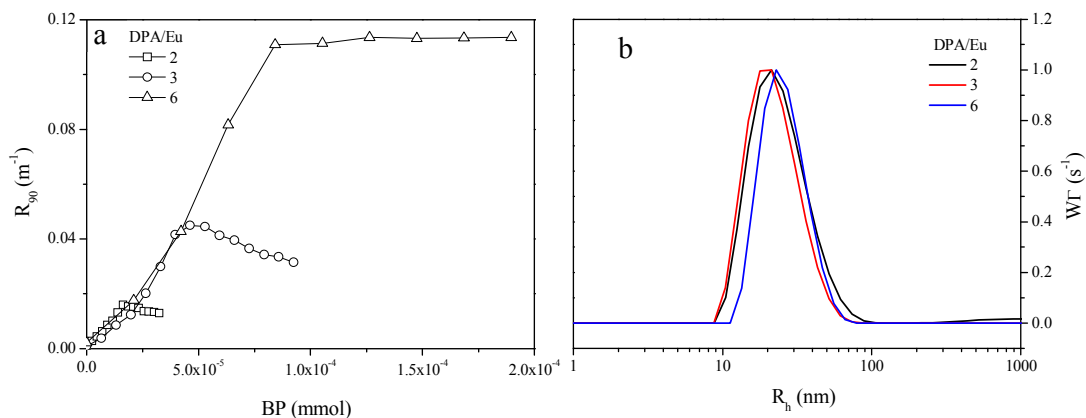


Figure 1 a: Light scattering titration of Eu-L₂EO₄ coordination structures at different DPA/Eu ratio; the intensity is represented at excess Rayleigh ratio and is plotted as a function of amount of P2MVP₄₁-*b*-PEO₂₀₅ added. b: CONTIN analysis of the size and size distribution of Eu-C3Ms at different DPA/Eu ratios. The micelles are prepared in 20 mM MES buffer at pH 6, and Eu(III) concentration is fixed at 0.5 mM.

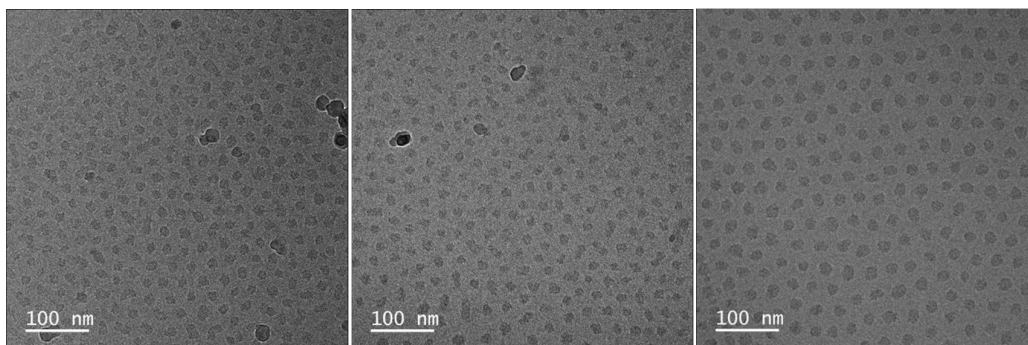
Figure 2

Figure 2 Cryo-TEM images of Eu-C3Ms. From left to right, the DPA/Eu ratio changes from 2 to 3, to 6.

Table 1

DPA/Eu	N_{LS}	f_{ligand} (%)	R_h (nm)	R_{core} (nm)	H_{shell} (nm)	Aggregation Number			$\tau_{\text{H}_2\text{O}}$ (ms)	$\tau_{\text{D}_2\text{O}}$ (ms)	q_{average}
						Eu	L_2EO_4	BP			
2	1.1	-	21	7	14	910	910	25	0.67	2.66	1.04
3	3.1	-	21	7	14	413	620	37	1.18	2.70	0.27
6	6.2	12	24	9	15	293	663	48	1.78	2.53	-0.1 ^a

Table 1 Summary of the parameters related to coordination structure and formed micelles. N_{LS} is the charge number per Eu(III)-coordination unit based on the light scattering titration. f_{ligand} : fraction of free ligand in solution; R_h : hydrodynamic radius; R_{core} : core radius; H_{shell} : shell thickness. τ : life time of Eu-C3Ms ($\lambda_{\text{ex}}=395$ nm, $[\text{Eu}] = 0.5$ mM). q_{average} : average number of inner sphere water molecules. ^a: corresponding to $q_{\text{average}} = 0$ within the error range, see ref. 20. Data fitting and calculations are in Supporting Information.

Figure 3

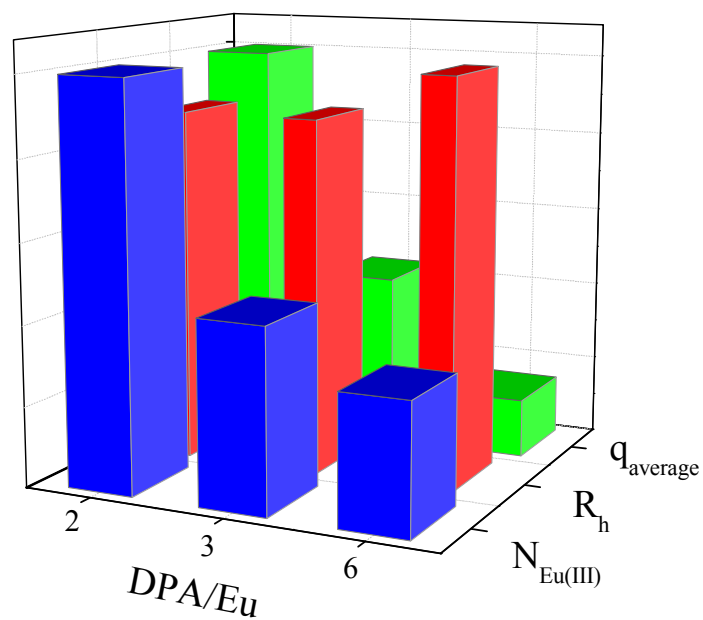


Figure 3 Variations of the normalized hydrodynamic radius (R_h), number of Eu(III) within one micelles ($N_{Eu(III)}$) and the average number of inner sphere water molecules ($q_{average}$) at different DPA/Eu ratio. For details on data analysis, calculations and the absolute numbers, see Table 1 and Supporting Information.

Figure 4

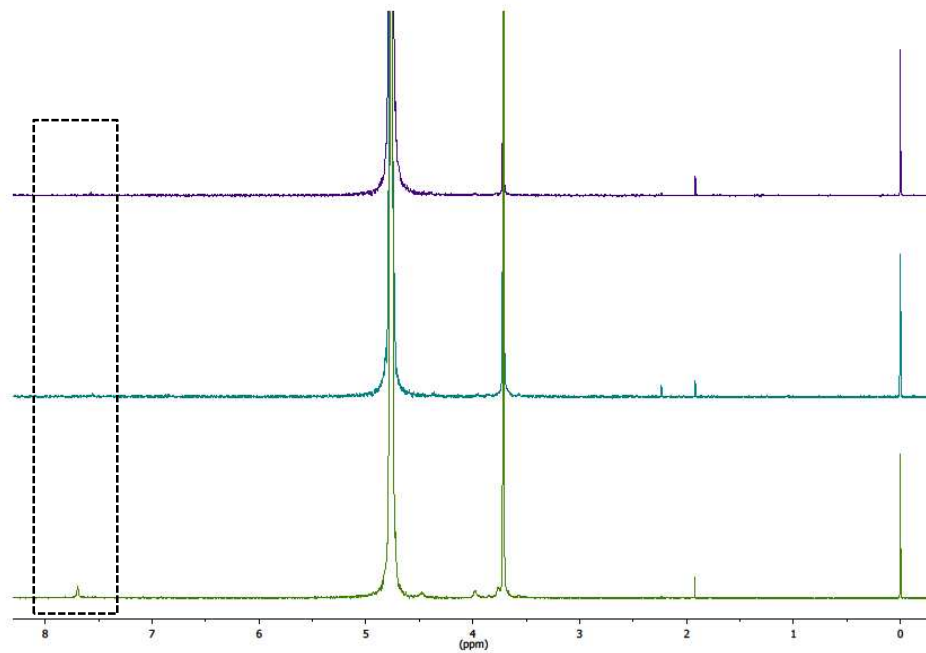


Figure 4 ^1H -NMR spectrum of the Eu-C3Ms at different DPA/Eu ratio. TSP is applied as an internal standard. DPA/Eu ratio are 2, 3, 6 from top to bottom.

Figure 5

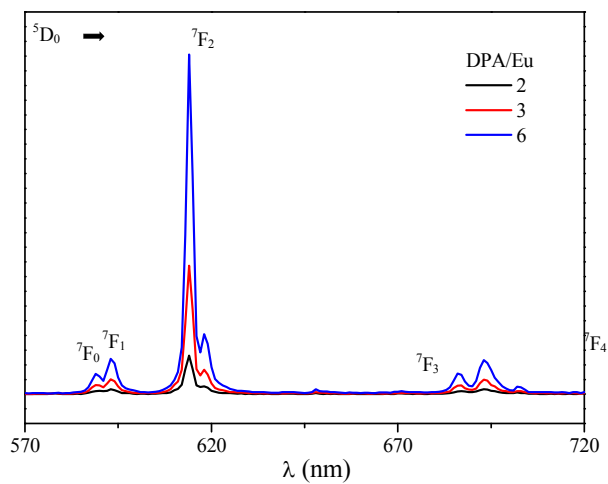


Figure 5 Luminescence emission of Eu-C3Ms prepared at different DPA/Eu ratio. (λ_{ex} = 395 nm, [Eu] = 0.5 mM, in 20 mM MES buffer at pH 6).

Figure 6

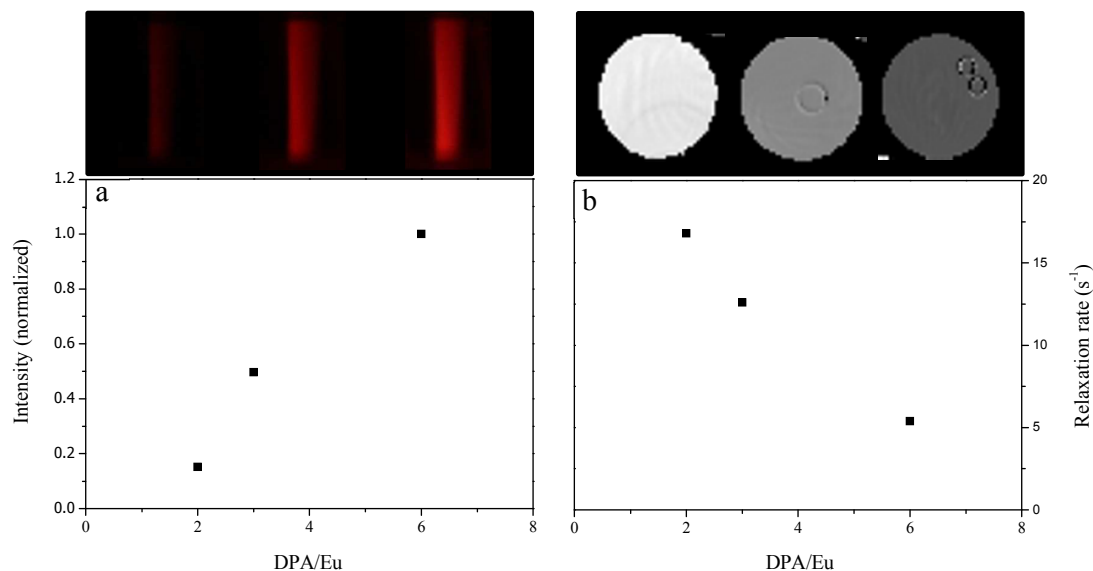


Figure 6 a: Luminescence emission intensity (614 nm) of Eu-C3Ms at different DPA/Eu ratios normalized by the highest intensity at DPA/Eu ratio of 6. (λ_{exc} : 395 nm for spectrum and 295 nm (xenon lamp) for the image). b: T₁-map MR images (at 3 T) and relaxation rates (at 0.7 T) of Gd-C3Ms at different DPA/Gd ratio ([Gd]: 0.5 mM). The small rings in the images are from the glass capillaries used to distinguish the different solutions.

Figure 7

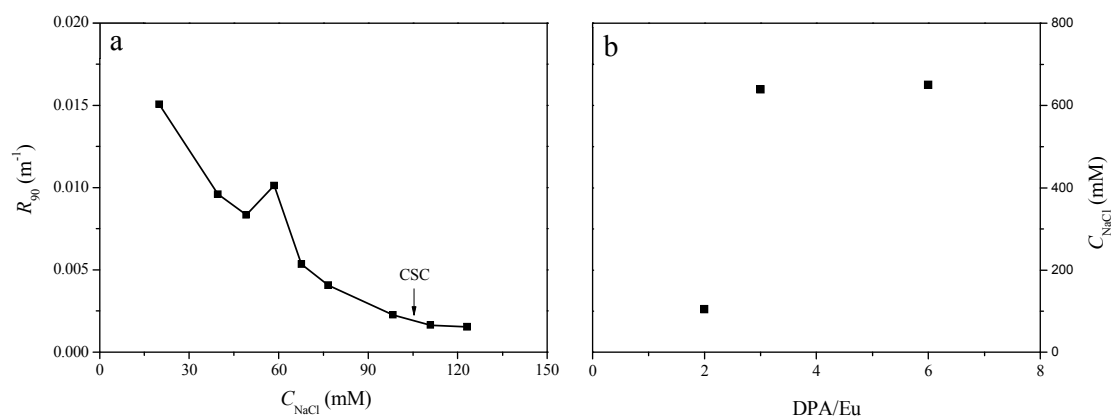


Figure 7 a: Intensity decay upon adding NaCl into Eu-C3Ms solution at DPA/Eu of 2, micelles at other ratios show similar titration curves (Supporting Information). b: CSC (critical salt concentration, indicated by the arrow) of Eu-C3Ms prepared at different DPA/Eu ratio.

References:

1. M. Elsabahy and K. L. Wooley, *Chem. Soc. Rev.*, 2012, **41**, 2545-2561.
2. F. Zaera, *Chem. Soc. Rev.*, 2013, **42**, 2746-2762.
3. T. Lammers, S. Aime, W. E. Hennink, G. Storm and F. Kiessling, *Acc. Chem. Res.*, 2011, **44**, 1029-1038.
4. J. During, A. Holzer, U. Kolb, R. Branscheid and F. Grohn, *Angew. Chem.-Int. Edit.*, 2013, **52**, 8742-8745.
5. J. C. G. Bunzli and C. Piguet, *Chem. Rev.*, 2002, **102**, 1897-1928.
6. M. Bottrill, L. K. Nicholas and N. J. Long, *Chem. Soc. Rev.*, 2006, **35**, 557-571.
7. D. D. Castelli, E. Gianolio, S. G. Crich, E. Terreno and S. Aime, *Coord. Chem. Rev.*, 2008, **252**, 2424-2443.
8. C. M. G. dos Santos, A. J. Harte, S. J. Quinn and T. Gunnlaugsson, *Coord. Chem. Rev.*, 2008, **252**, 2512-2527.
9. L. Pellegatti, J. Zhang, B. Drahos, S. Villette, F. Suzenet, G. Guillaumet, S. Petoud and E. Toth, *Chem. Commun.*, 2008, 6591-6593.
10. J. C. G. Bunzli, *Chem. Rev.*, 2010, **110**, 2729-2755.
11. Y. Y. Mai and A. Eisenberg, *Acc. Chem. Res.*, 2012, **45**, 1657-1666.
12. Z. S. Ge and S. Y. Liu, *Chem. Soc. Rev.*, 2013, **42**, 7289-7325.
13. J. L. Turner, D. P. J. Pan, R. Plummer, Z. Y. Chen, A. K. Whittaker and K. L. Wooley, *Adv. Funct. Mater.*, 2005, **15**, 1248-1254.
14. Y. Y. Li, H. Cheng, Z. G. Zhang, C. Wang, J. L. Zhu, Y. Liang, K. L. Zhang, S. X. Cheng, X. Z. Zhang and R. X. Zhuo, *ACS Nano*, 2008, **2**, 125-133.
15. C. S. Bonnet, L. Pellegatti, F. Buron, C. M. Shade, S. Villette, V. Kubicek, G. Guillaumet, F. Suzenet, S. Petoud and E. Toth, *Chem. Commun.*, 2010, **46**, 124-126.
16. K. Shiraiishi, K. Kawano, Y. Maitani and M. Yokoyama, *J. Control. Release*, 2010, **148**, 160-167.
17. D. Parker, *Coord. Chem. Rev.*, 2000, **205**, 109-130.
18. J. Wang, A. H. Velders, E. Gianolio, S. Aime, F. J. Vergeldt, H. Van As, Y. Yan, M. Drechsler, A. de Keizer, M. A. Cohen Stuart and J. van der Gucht, *Chem. Commun.*, 2013, **49**, 3736-3738.
19. T. Vermonden, W. M. de Vos, A. T. M. Marcelis and E. J. R. Sudholter, *Eur. J. Inorg. Chem.*, 2004, 2847-2852.
20. T. Vermonden, J. van der Gucht, P. de Waard, A. T. M. Marcelis, N. A. M. Besseling, E. J. R. Sudholter, G. J. Fleer and M. A. C. Stuart, *Macromolecules*, 2003, **36**, 7035-7044.
21. Y. Yan, N. A. M. Besseling, A. de Keizer, A. T. M. Marcelis, M. Drechsler and M. A. C. Stuart, *Angew. Chem.-Int. Edit.*, 2007, **46**, 1807-1809.
22. J. Wang, I. K. Voets, R. Fokkink, J. van der Gucht and A. H. Velders, *Soft Matter*, 2014, **10**, 7337-7345.
23. s. S. I. DPA/Ln ratio of 10 was also studied but those data are similar to the ones presented for 6.
24. Y. Yan, N. A. M. Besseling, A. de Keizer and M. A. C. Stuart, *J. Phys. Chem. B*, 2007, **111**, 5811-5818.
25. Y. Yan and J. B. Huang, *Coord. Chem. Rev.*, 2010, **254**, 1072-1080.
26. S. van der Burgh, A. de Keizer and M. A. Cohen Stuart, *Langmuir*, 2004, **20**, 1073-1084.
27. J. R. Lakowicz, *Principles of Fluorescence Spectroscopy*, 3rd Ed; Springer: New York, 2006; p 55-57.
28. J. Andres and A. S. Chauvin, *Eur. J. Inorg. Chem.*, 2010, 2700-2713.
29. A. Beeby, I. M. Clarkson, R. S. Dickins, S. Faulkner, D. Parker, L. Royle, A. S. de Sousa, J. A. G. Williams and M. Woods, *J. Chem. Soc.-Perkin Trans. 2*, 1999, 493-503.
30. A. S. Chauvin, F. Gummy, D. Imbert and J. C. G. Bunzli, *Spectr. Lett.*, 2004, **37**, 517-532.
31. L. M. Xu, Y. Y. Jing, L. Z. Feng, Z. Y. Xian, Y. Yan, Z. Liu and J. B. Huang, *Phys. Chem. Chem. Phys.*, 2013, **15**, 16641-16647.
32. L. M. Xu, L. Z. Feng, Y. C. Han, Y. Y. Jing, Z. Y. Xian, Z. Liu, J. B. Huang and Y. Yan, *Soft Matter*, 2014, **10**, 4686-4693.
33. A. L. Gassner, C. Duhot, J. C. G. Bunzli and A. S. Chauvin, *Inorg Chem*, 2008, **47**, 7802-7812.
34. X. F. Yuan, A. Harada, Y. Yamasaki and K. Kataoka, *Langmuir*, 2005, **21**, 2668-2674.
35. Y. Yan, A. de Keizer, M. A. Cohen Stuart, M. Drechsler and N. A. M. Besseling, *J. Phys. Chem. B*, 2008, **112**, 10908-10914.
36. Y. Yan, N. A. M. Besseling, A. de Keizer, M. Drechsler, R. Fokkink and M. A. Cohen Stuart, *J. Phys. Chem. B*, 2007, **111**, 11662-11669.
37. H. M. van der Kooij, E. Spruijt, I. K. Voets, R. Fokkink, M. A. Cohen Stuart and J. van der Gucht, *Langmuir*, 2012, **28**, 14180-14191.
38. J. Y. Wang, A. de Keizer, R. Fokkink, Y. Yan, M. A. Cohen Stuart and J. van der Gucht, *J. Phys. Chem. B*, 2010, **114**, 8313-8319.
39. Y. Sun, X. J. Zhu, J. J. Peng and F. Y. Li, *ACS Nano*, 2013, **7**, 11290-11300.
40. J. Rieffel, C. F., J. Kim, G. Y. Chen, W. Shao, S. Shao, U. Chitgupi, R. Hernandez, S. A. Graves, R. J. Nickles, P. N. Prasad, C. Kim, W. B. Cai and J. F. Lovell, *Adv. Mater.*, 2015, **27**, 1785-1790.

Revealing and tuning the core, structure, properties and function of polymer micelles with lanthanide-coordination complexes

Junyou Wang,^a Andrea Groeneveld,^a Maria Oikonomou,^a Alena Prusova,^b Henk Van As,^b Jan van Lent,^c Aldrik H. Velders^{a,d*}

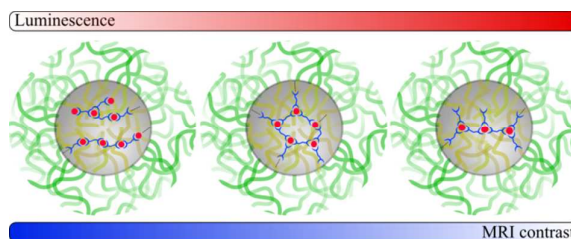
a: Laboratory of BioNanoTechnology, Wageningen University, Dreijenplein 6, 6703 HB Wageningen, The Netherlands

b: Laboratory of Biophysics and Wageningen NMR Centre, Wageningen University, Dreijenplein 3, 6703 HA Wageningen, The Netherlands

c: Wageningen Electron Microscopy Centre, Wageningen University, Droevendaalsesteeg 1, 6708 PB Wageningen, The Netherlands

d: Interventional Molecular Imaging Laboratory, Department of Radiology, Leiden University Medical Centre, Leiden, The Netherlands.

Table of contents entry



Lanthanide [Eu(III) and Gd(III)] incorporated micelles with tunable coordination structures and corresponded functions have been prepared and investigated.